FT-Raman, FT-IR, NMR structural characterization and antimicrobial activities of 1,6-bis(benzimidazol-2-yl)-3,4-dithiahexane ligand and its Hg(II) halide complexes

ARTICLE *in* STRUCTURAL CHEMISTRY · FEBRUARY 2007

Impact Factor: 1.84 · DOI: 10.1007/s11224-007-9253-z

Struct Chem (2008) 19:71–80
DOI 10.1007/s11224-007-9253-z

ORIGINAL PAPER

FT-Raman, FT-IR, NMR structural characterization and antimicrobial activities of 1,6-bis(benzimidazol-2-yl)-3,4-dithiahexane ligand and its Hg(II) halide complexes

Naz Mohammed Aghatabay · Metin Tulu · Yaghub Mahmiani · Mehmet Somer · Basaran Dulger

Received: 6 June 2007 / Accepted: 21 September 2007 / Published online: 26 October 2007

Abstract 1,6-Bis(benzimidaz-2-yl)-3,4-dithiahexane ligand (L) and its mercury halide complexes were prepared and characterised. The elemental analysis, molecular conductivity, FT-Raman, FT-IR (mid, far), ^{1}H, ^{13}C NMR and geometry optimization in MOPAC using MNDOd parameter on CACHE, prove the existence of neutral, mononuclear and the distorted tetrahedral $[Hg(L)X_2]$ complexes. In all the three complexes, the ligand acts as a chelating bidentate, through two of the bridging sulphur atoms and together with the monodentate coordination of the two anionic halide ligands to the metal centre forming a possible 4-coordinate compounds. The antimicrobial activities of free ligand, its hydrochlorinated salt, mercury halides and the complexes are evaluated using disk diffusion method in dimethyl sulfoxide (DMSO) as well as the minimal inhibitory concentration (MIC) dilution method, against 10 bacteria. The obtained results from disk diffusion method are assessed in side-by-side comparison with those of Penicillin-g, Ampicillin, Cefotaxime, Vancomycin, Oflaxacin and Tetracyclin well-known antibacterial agents. The results from dilution procedure are compared with Gentamycin as antibacterial and Nystatin as antifungal. The antifungal activities are reported on five yeast cultures namely *Candida albicans*, *Kluyveromyces fragilis*, *Rhodotorula rubra*, *Debaryomyces hansenii* and *Hanseniaspora guilliermondii*, and the results are referenced with Nystatin, Ketaconazole and Clotrimazole, commercial antifungal agents. In most cases, the compounds show broad-spectrum ($Gram^{+}$ & $Gram^{-}$ bacteria) activities that are comparatively, slightly less active or equipotent to the antibiotic and antifungal agents in the comparison tests.

Keywords Antimicrobial · Bidentate · Chelating · Disk diffusion · Gentamycin · Raman

N. M. Aghatabay (✉) · M. Tulu · Y. Mahmiani
Department of Chemistry, Fatih University, Büyükçekmece, Istanbul 34500, Turkey
e-mails: natabay@fatih.edu.tr; natabay@yahoo.com

M. Somer
Department of Chemistry, Koç University, Rumelifeneri Yolu, Sariyer, Istanbul 34450, Turkey

B. Dulger
Department of Biology, Canakkale Onsekiz Mart University, Canakkale, Turkey

Introduction

Following successful therapeutical applications of platinum complex cisplatin as an antitumour drug and gold complex auranofin as an antirheumatic drug, a large number of complexes with other metals have been studied and, in several cases, subjected to clinical tests [1–8]. In this expanding field, the interest towards transition metal complexes containing hetero-donor ligands has increased in order to obtain metal-based drugs either exhibiting a high biological activity together with a reduced toxicity or reduced biological activity for metal ion detoxification. In this respect, benzimidazole derivatives together with their transition metal complexes have been extensively investigated [9–14].

Metal ions are required for many critical functions in humans. Scarcity of some metal ions can lead to disease. Well-known examples include pernicious anaemia resulting from iron deficiency, growth retardation arising from insufficient dietary zinc and heart disease in infants owing to copper deficiency. Metal ions can also induce toxicity in humans, classic examples being heavy metal poisons such

as mercury, antimony and lead. Toxicity can arise from excessive quantities of either an essential metal, possibly the result of a metabolic deficiency, or a nonessential metal. Both acute and chronic exposure can be treated by chelation therapy, in which theoretical assumptions such as the Irving–Williams series of stability [15] and hard–soft acid–base principle of Pearson–Parr [16] are useful in the choice of chelating agent. Since chelating ligands can also remove essential metals not present in toxic amounts, ligands with high specificity are greatly desired. Understanding the bioinorganic chemistry and molecular biology of natural detoxification mechanisms, and designing and applying ion-specific chelating agents to treat metal overloads, are two components of a major aspect of the new science that is evolving at the interface of biocoordination chemistry and medicine.

Mercury ions are soft acids with very high toxicity. One of the best illustrations of this metal ion principle in biochemistry is provided by the metallothionein. Metallothionein is a generic name for a super family of ubiquitous low molecular weight metalloproteins possessing a unique type of sulphur-based metal cluster. Vital roles for this pleiotropic protein result in its involvement in homoeostasis of essential trace metals such as zinc, or sequestration of the nonessential toxic metals such as mercury and cadmium. In this respect, the thiophilic potentiality of Hg(II) may provide the scope for treatment of mercury poisoning with sulphur donor ligand such as, 6-bis(3-benzimidazyl)-3,4-dithiahexane by chelating the metal ion through their sulphur functions and thus promoting its elimination. In the present report, we focus upon the synthesis, physicochemical characterization and pharmacological investigation of the ligand, its hydrochloride salt, mercury halides and $[Hg(L)X_2]$ complexes.

Experimental

Materials and methods

All chemicals and solvents were reagent grade and were used without further purification. Purity of the compounds was tested on thin layer chromatography (t.l.c.) plates (silica gel 60 F_{254} Merck). Melting points were determined with Electro-thermal 9,100 melting point apparatus. Analytical data were obtained with Carlo Erba 1,106 analyser. Molar conductivity of the complexes was measured on a WPA CMD750 conductivity meter in dimethyl sulfoxide (DMSO) solution at 25 °C temperature. FT-IR spectra were recorded (mid as KBr pellets and far in polyethylene tablets) on a Jasco FT/IR-600 Plus Spectrometer. FT-Raman spectra were obtained from powdered samples placed in a Pyrex tube using the Bruker RFS 100/S spectrometer in the range 4,000–20 cm^{-1}. The samples were excited by a near IR Nd: YAG laser, delivering an excitation wavelength of 1,064 nm, 150–200 mW. Routine ^{1}H and ^{13}C NMR spectra are recorded at ambient temperature, on a 500 MHz NMR Spectrometer in deuterated (DMSO-d_6). Chemical shifts (δ) are expressed in units of ppm. relative to TMS. The ligand (L) is prepared following published procedures [17, 18].

Theoretical calculation

The structure of the ligand and the $[Hg(L)Cl_2]$ complex (Figs. 1 and 2) were refined by performing a geometry optimization calculation in MOPAC using MNDOd parameter available on CACHE work system pro version 6.1.10 package program. Because of the structural analogy, the results could be directly transferred to the bromo and iodo complexes. The geometry optimization of $[Hg(L)Cl_2]$ yields a highly distorted tetrahedral environment around Hg ion (i.e. $d(Hg–Cl_a) = 2.3747$, $d(Hg–Cl_b) = 2.3743$, $d(Hg–S_a) = 2.5671$, $d(Hg–S_b) = 2.5658$ Å and; bond angles $\angle Cl–Hg–Cl = 140.4196$, $\angle S_a–Hg–Cl_a = 109.8542$, $\angle S_a–Hg–Cl_b = 106.3389$, $\angle S_b–Hg–Cl_b = 110.0540$ and $\angle S_b–Hg–Cl_a = 106.0443°$. The calculated (S–S) bond lengths for the free ligand and the complex are directly comparable: d(S–S) = 2.0036 Å (ligand) and d(S–S) = 2.0633 Å (complex).

Synthesis

1,6-Bis(3-benzimidazyl)-3,4-dithiahexane (L)

The ligand was synthesised using a mixture of 3,3′-dithiodipropionic acid (3.9 g, 18.6 mmol) and freshly sublimed *o*-phenylenediamine (4 g, 37.1 mmol) in 5 M HCl (40 cm^3) refluxing for 48 h. The cooled precipitates were collected and identified as (L)·2HCl. The free base ligand

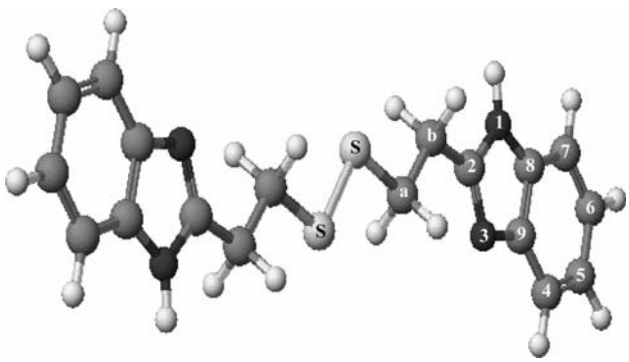

Fig. 1 Proposed structure of ligand (L)

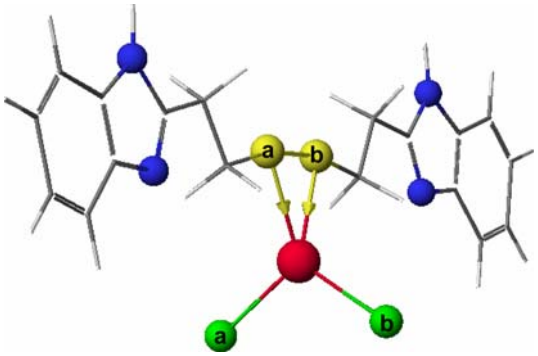

Fig. 2 Optimised structure of $[Hg(L)Cl_2]$ complex

(L) was obtained by treatment of (L)·2HCl with an aqueous 5% ammonia solution. The yellowish precipitate was decolourised with charcoal in EtOH at reflux temperature, recrystallised from EtOH giving a pale yellow solid (4.90 g, 70%). Decompose at 172 °C.

Complexes

A general procedure for the synthesis of complexes is described as follows: An equivalent mixture of mercury halide and the corresponding ligand in EtOH was stirred for couple of hours at room temperature. The resulting precipitate was collected, washed several times with small portions of ethanol to render it pure and dried under vacuum.

$[Hg(L)Cl_2]$ $2H_2O$ (white 280 mg, 75%). Decompose 186 °C. Found (calculated): C, 31.87 (32.63); H, 3.66 (3.32); N, 7.84 (8.45); 10.36 (9.67) $[C_{18}H_{22}N_4O_2S_2HgCl_2]$. The molar conductivity was 6.4 Ω^{-1} cm^2 mol^{-1}.
$[Hg(L)Br_2]$ H_2O (white, 320 mg, 78%). Decompose 189 °C. Found (calculated: C, 29.93 (29.47); H, 2.85 (2.73); N, 7.32 (7.64); 9.10 (8.73) $[C_{18}H_{20}N_4OS_2HgBr_2]$. Molar conductivity was 5.8 Ω^{-1} cm^2 mol^{-1}.
$[Hg(L)I_2]$ $2H_2O$ (pale yellowish, 150 mg, 60%). Decompose 178 °C. Found (calculated): C, 25.10 (25.53); H, 2.87 (2.60); N, 6.78 (6.62); 7.47 (7.56) $[C_{18}H_{22}N_4O_2S_2HgI_2]$. Molar conductivity was 9.1 $\Omega^{-1}cm^2$ mol^{-1}.

Pharmacology

Microorganisms

The antimicrobial activities are evaluated against Gram positive *(Staphylococcus aureus* ATCC 6538, *Bacillus cereus* ATCC 7064, *Mycobacterium smegmatis* CCM 2067, *Listeria monocytogenes* ATCC 15313, *Micrococcus luteus* La 2971) and Gram negative (*Escherichia coli* ATCC 11230, *Klebsiella pneumoniae* UC57, *Pseudomonas aeruginosa* ATCC 27853, *Proteus vulgaris* ATCC 8427, *Enterobacter aerogenes* ATCC 13048) bacteria and the yeast cultures (*Candida albicans* ATCC 10231, *Kluyveromyces fragilis* NRRL 2415, *Rhodotorula rubra* DSM 70403, *Debaryomyces hansenii* DSM 70238 and *Hanseniaspora guilliermondii* DSM 3432) using both disk diffusion method [19, 20] and measuring the (MIC) determined by the broth dilution method [21]. Both methods are outlined fully in the experimental sections.

Biological data

Standardised samples of Penicillin-g (blocking the formation of bacterial cell walls, rendering bacteria unable to multiply and spread; Ampicillin (penetrating and preventing the growth of Gram-negative bacteria); Cefotaxime (used against most Gram-negative enteric bacteria); Vancomycin (acting by interfering with the construction cell walls in bacteria), Ofloxacin (entering the bacterial cell and inhibiting DNA-gyrase, which is involved in the production of genetic material, preventing the bacteria from reproducing); Tetracyclines (exerting their antimicrobial effect the inhibition of protein synthesis; Nystatin (binding to sterols in the fungal cellular membrane altering the permeability to allow leakage of the cellular contents and destroying the fungus); Ketoconazole (inhibiting the growth of fungal organisms by interfering with the formation of the fungal cell wall) and Clotrimazole (interfering with their cell membranes and causing essential constituents of the fungal cells leakage). Mueller Hinton media, Nutrient Broth and Malt Extract Broth are purchased from Difco and yeast extracts is obtained from Oxoid.

Disk diffusion method

Screening for antibacterial and antifungal activities are carried out using sterilised antibiotic discs (6 mm), following the procedure performance standards for Antimicrobial Disk Susceptibility Tests, outlined by the National Committee for Clinical Laboratory Standards—NCCLS [19, 20].

Fresh stock solutions (30 μg mL^{-1}) of the ligands and the complexes are prepared in freshly distilled dimethyl sulfoxide (DMSO) according to the needed concentrations for the experiments. The compounds are quite soluble in DMSO (not soluble in water) and do not show any decomposition in this solvent (checked by ^1H and ^{13}C

NMR spectra in DMSO-d_6). To ensure that the solvent had no effect on bacterial growth, a control test was performed with test medium supplemented with DMSO as same procedures as used in the experiments. Sterilised antibiotic discs having a diameter of 6 mm (Schleicher & Schull No 2668, Germany) are impregnated with 20 μL of these solutions. All the bacteria are incubated and activate at 30 °C for 24 h inoculation into Nutrient Broth (Difco), and the yeasts are incubated in Malt Extract Broth (Difco) for 48 h. Inoculums containing 10^6 bacterial cells or 10^8 yeast cells per mL are spread on Mueller-Hinton Agar (Oxoid) plates (1 mL inoculum for each plate). The discs injected with solutions are placed on the inoculated agar by pressing slightly and incubated at 35 °C (24 h) and at 25 °C (72 h) for bacteria and yeast, respectively. On each plate on appropriate reference antibiotic disc is applied depending on the test micro-organisms. In each case triplicate tests are performed and the average is taken as final reading.

Dilution method

Screening for antibacterial and antifungal activities were carried out by preparing a broth micro dilution, following the procedure outlined in Manual of Clinical Microbial [21]. All the bacteria were incubated and activated at 30 °C for 24 h inoculation into Nutrient Broth, and the yeasts were incubated in Malt Extract Broth for 48 h. The compounds were dissolved in DMSO (2 mg mL^{-1}) and then diluted using caution adjusted Mueller Hinton Broth (Oxoid). Two-fold serial concentrations of the compounds were employed to determine the (MIC) ranging from 200 μg mL^{-1} to 1.56 μg mL^{-1}.

Cultures were grown at 37 °C (20 h) and the final inoculation (inoculums) was approximately 10^6 cfu mL^{-1}. Test cultures were incubated at 37 °C (24 h). The lowest concentrations of antimicrobial agents that result in complete inhibition of microorganisms were represented as (MIC) μg mL^{-1}. In each case, triplicate tests were performed and the results are expressed as means.

Results and discussion

Nuclear magnetic resonance

The ^{1}H-n.m.r. spectra pattern do not change significantly due to the complex formation compared with free ligand. Broad and unresolved imine proton atoms for the ligand and the complexes are observed as expected in the 10–13 ppm. spectral regions. This may be taken as evidence that the bis-3 and 3′ nitrogen atoms in the imine ring are not playing any role in the coordination sphere. If nitrogen atoms are coordinated to the metal centre, this should have caused inhibition of the fluxional behaviour of imine's proton atoms, giving well resolved signals as were the case for palladium complexes [18]. No significant changes are observed for aromatic ring protons (4,7) and (5,6). This supports that coordination may occur only through sulphur atoms.

Significant changes are observed in bridging CH_{2a} and CH_{2b} protons in the complexes (Table 1). This supports the contention that the both sulphur atoms are playing an important role in the coordination sphere.

As expected, the ^{13}C-n.m.r. spectrum of the benzimidazole ring of the ligand exhibits four signals due to the fluxional behaviour of the imine proton. No significant changes are observed upon complexation in this region of spectrum. This indicates that the fluxional behaviour of the imine protons was not inhibited due to complex formation, which also supports the idea that coordination occurs via sulphur atoms to the metal centre. A considerable amount of changes are observed for the bridging aliphatic carbon atoms upon complex formation, particularly on the CH_2

Table 1 ^{1}H and ^{13}C NMR data of the ligand (L) and the $Hg(L)X_2$ complexes

^{1}H NMR	CH_{2a}	CH_{2b}	4,7	5,6	NH	
Ligand	2.98 (t, 4H)	2.72 (t, 4H)	7.23 (m, 4H)	7.52 (m, 4H)	10–13 (v.b, 2H)	
$Hg(L)Cl_2$	3.39 (t, 4H)	3.22 (t, 4H)	7.27 (m, 4H)	7.74 (m, 4H)	10–12 (v.b, 2H)	
$Hg(L)Br_2$	3.38 (t, 4H)	3.19 (t, 4H)	7.26 (m, 4H)	7.76 (m, 4H)	11–13 (v.b, 2H)	
$Hg(L)I_2$	3.36 (t, 4H)	3.24 (t, 4H)	7.27 (m, 4H)	7.64 (m, 4H)	9–10 (v.b, 2H)	
^{13}CNMR	C_a	C_b	4,7	5,6	8,9	2
Ligand	35.56	28.46	114.93	123.59	136.49	153.32
$Hg(L)Cl_2$	37.10	29.30	115.90	124.25	138.05	155.60
$Hg(L)Br_2$	35.85	27.90	114.65	122.70	136.95	154.20
$Hg(L)I_2$	36.45	29.00	115.95	124.18	137.85	155.25

t, triplet; m, multiplet; v.b, very broad

adjacent to the sulphur atoms. The resonance shifts from δ 35.55 for the free ligand to 37.10, 35.85 and 36.45 ppm. for $Hg(L)X_2$ (X = Cl, Br and I) complexes, respectively. The downfield resonances, most probably caused by deshielding effects by the sulphur atoms, which also tends to support that the coordination occurs via the sulphur atoms rather than nitrogen atoms. Full n.m.r. spectra data and their assignments are presented in Table 1.

Vibrational spectra

The characteristic νCH and δCH modes of ring residues and aliphatic groups are observed in wave region between 3,100–2,850 cm^{-1} and 1,400–950 cm^{-1}, both in i.r. and Raman for the ligand and complexes. Slight but specific differences between spectra of the free ligand and the complexes in this region show strong support for the formation of new complexes particularly on the ν(CH) modes of CH_2 residues (Figs. 3, 4; Tables 2, 3).

Appearance of a strong broad band at ca. 3,250 cm^{-1} in the i.r. spectra of the complexes may be due to combination of lattice water ν(H–O–H) and imine ν(N–H) vibration

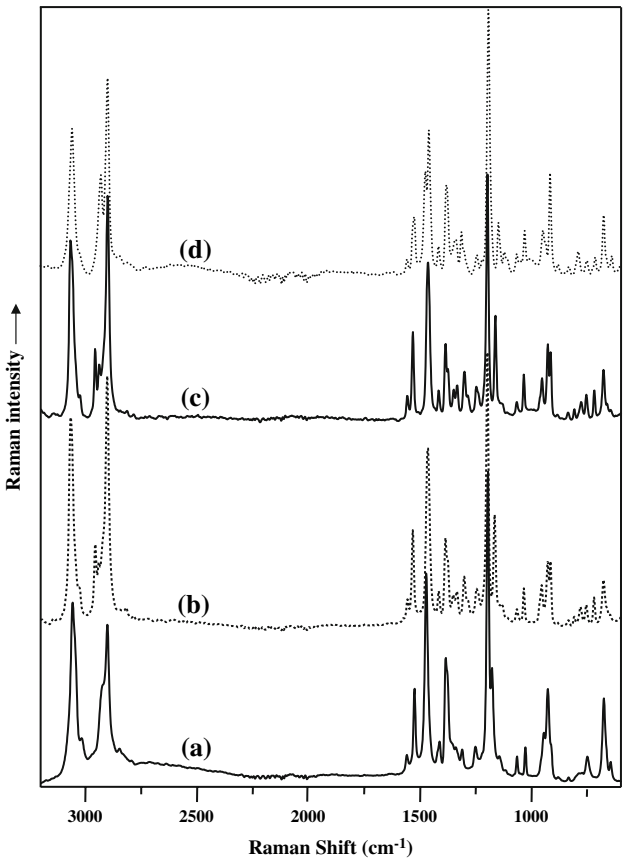

Fig. 3 Raman spectrum of **(a)** (L), **(b)** $[Hg(L)Cl_2]$, **(c)** $[Hg(L)Br_2]$ and **(d)** $[Hg(L)I_2]$ in the 3,200–700 cm^{-1} region

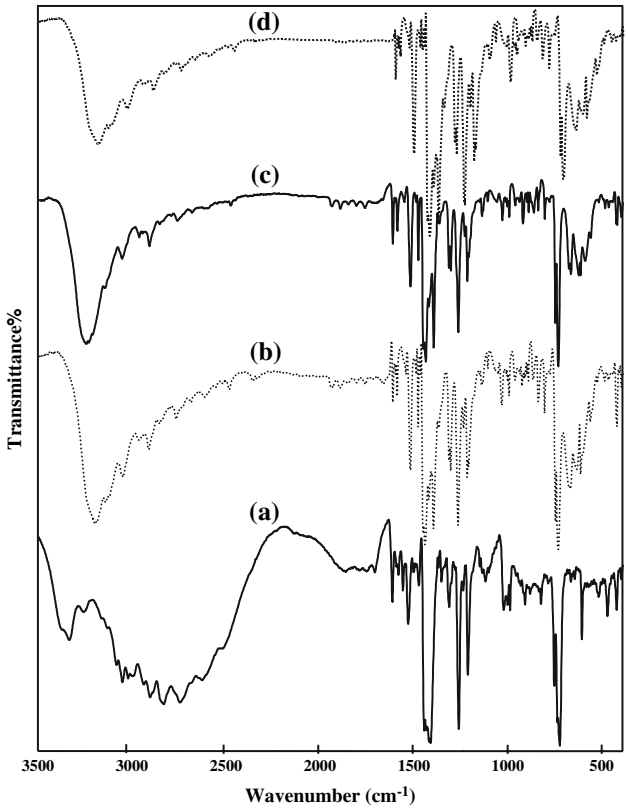

Fig. 4 Infrared spectrum of **(a)** (L), **(b)** $[Hg(L)Cl_2]$, **(c)** $[Hg(L)Br_2]$ and **(d)** $[Hg(L)I_2]$ in the 3,500–400 cm^{-1} region

frequencies (antisymmetric and symmetric OH and NH stretching). The low frequency appearance of ν(H–O–H) probably caused by double intermolecular hydrogen bonding between the hydrate water molecule and imine nitrogen atoms. The bending vibrations for δ(H–O–H) and δ(N–H) groups are observed at ca. 1,600 and 1,450 cm^{-1}, respectively (Table 2).

As reported previously, the 1,3-bis(benzimidazol-2-yl)-2-thiapropane and 1,6-bis(benzimidazol-2-yl)-3,4-dithiahexane (L) (Fig. 1) ligands have very similar molecular structures, differing only in the number of the bridging sulphur atoms [18, 22]. This fact is also reflected in their vibrational spectra resembling each other remarkably. The most significant difference occurs in the wave region around 500 cm^{-1} with the appearance of some new bands in the ligand (L) spectrum at 539, 522 and 491 cm^{-1} (Raman) and 500 and 489 cm^{-1} (i.r.). The vibrational frequency of an isolated S_2 molecule in the inert gas matrix (mat) is measured at 718 cm^{-1} [23, 24]. The $\nu(S_2)$ in the free-state (solid doped in KCl) is 623 cm^{-1} [25]. Most of the complexes containing $(S_2)^{2-}$ ligand undergo three types of coordination: as a monometallic chelate ring; bimetallic bridging via both sulphur atoms and bimetallic coordination through both sulphur atoms as monodentate ligand. In the present case, nitrogen and sulphur atoms are both competitors for

Table 2 Some prominent i.r. bands of ligand and $[Hg(L)X_2]$ complexes with their assignments

Ligand (L): 3,335, 3,260, ν[(N–H), (H–O–H)], 3,090 ν_{as}(C–H_{ar}), 3,056, 3,023 ν_s(C–H_{ar}), 2,940 ν_{as}(C–H), 2,907, 2,850 ν_s(C–H), 1,980–1,760 (aromatic patterns), 1,624 ν(C=C), 1,602 δ(H–O–H), 1,592 ν_{as}(C=N), 1,568, 1,541, 1,454–1,430 [ν_s(C=N), δ(N–H), ν(C–H)], 1,272 [ω(CH_2), ν(C–N)], 1,223, 765, 750–737 [δ(C–H_{ar}), δ(C=C)], 678 ν_{as}(S–C), 618 ν_s(S–C), 528 ν(S–S), 486, 434, 361, 337, 309, 270, 242, 220, 206, 197, 190, 180

Hg(L)Cl2: 3,200, 3,143 ν[(N–H), 1,606 (H–O–H)], 3,121 ν_{as}(H–C_{ar}), 3,055 ν_s(H–C_{ar}), 2,969 ν_{as}(C–H), 2,915 ν_s(C–H), 1,960–1,780 (aromatic patterns), 1,620 ν(C=C), 1,606 δ(H–O–H), 1,589 ν_{as}(C=N), 1,528, 1,450 [ν_s(C=N), δ(N–H), ν(C–H)], 1,404, 1,275 [ω(CH_2), ν(C–N)] 1,225, 759, 744 δ(C=C_{ar}), 678, 645 ν_{as}(S–C), 625 ν_s(S–C), 573 ν_s(S–C), 498 ν(S–S), 434, 409, 353, 318, 278 ν(S–Hg–S), 253, 248 ν(Hg–Cl), 229, 221, 213, 202, 190, 180

Hg(L)Br_2: 3,247–3,145 ν[(N–H), (H–O–H)], 3,056, ν(C–H_{ar}), 2,966 ν_{as}(C–H), 2,910 ν_s(C–H), 1,950–1,770 (aromatic patterns), 1,620 ν(C=C), 1,606 δ(H–O–H), 1,596 ν_{as}(C=N), 1,526, 1,457–1,445 [ν_s(C=N), δ(N–H), ν(C–H)], 1,404, 1,273 [ω(CH_2), ν(C–N)], 759–743 [δ(C–H_{ar}), δ(C=C)], 668, 674, 634 ν_{as}(S–C), 625 ν_s(S–C), 601, 571, 505 ν(S–S), 432, 407, 354, 313, 278 ν(S–Hg–S), 255, 247 , 227, 214.202. 188 ν(Hg–Br)

Hg(L)I_2: 3,260 ν[(N–H), (H–O–H)], 3,100–3,050 [ν_{as}(C–H_{ar}), ν_s(C–H_{ar})], 2,945 ν_{as}(C–H), 2,920 ν_s(C–H), 1,980–1,800 (aromatic patterns), 624 ν(C=C), 1,587 ν_{as}(C=N), 1,570, 1,525, 1,484, 1,457–1,418 [ν_s(C=N), δ(N–H), ν(C–H)], 1,272–1,220 [ω(CH_2), ν(C–N)], 744 [δ(C–H_{ar}), δ(C=C)], 614, ν_{as}(S–C), 561, 551 ν_s(S–C), 523 ν(S–S), 472, 437, 411, 268 ν(S–Hg–S), 209

ν, stretching; δ, bending; ω, wagging

Table 3 Assignments of prominent Raman bands of the ligand and $[Hg(L)X_2]$ complexes

Ligand (L)	3,062 ν(C_a–H), 2,913 ν(CH_2), 1,623 ν(C=C), 1,590 ν_{as}(C=N), 1,540 ν_s(C=N), 1,455, 1,274 ω (CH_2), 774 δ(C=C_{ar}), 666 ν_{as}(S–C), 622 ν_s(S–C), 539, 522 ν(S–S), 491, 310, 273, 209, 179
Hg(L)Cl_2	3,069 ν(C_a–H), 2,965 ν(CH_2), 2,948 ν(CH_2), 2,913 ν(CH_2), 1,620 ν(C=C), 1,598 ν_{as}(C=N), 1,532 ν_s(C=N), 1,457, 1,276 ω (CH_2), 776 δ(C=C_{ar}), 682, 660 ν_{as}(S–C), 626 ν_s(S–C), 507ν(S–S), 497, 477, 315, 296 ν(S–Hg–S), 277, 250 ν(Hg–Cl), 185
Zn(L)Br_2	3,071 ν(C_a–H), 2,965 ν(CH_2), 2,948 ν(CH_2), 2,911 ν(CH_2), 1,620 ν(C=C), 1,596 ν_{as}(C=N), 1,530 ν_s(C=N), 1,455, 1,276 ω (CH_2), 776 δ(C=C_{ar}), 682, 660 ν_{as}(S–C), 626 ν_s(S–C), 506ν(S–S), 495, 477, 315, 292ν(S–Hg–S), 273, 175 ν(Hg–Br)
Zn(L)I_2	3,064 ν(C_a–H), 2,940 ν(CH_2), 2,911 ν(CH_2), ν(CH_2), 1,621 ν(C=C), 1,592 ν_{as}(C=N), 1,528 ν_s(C=N), 1,453, 1,272 ω (CH_2), 776 δ(C=C_{ar}), 670 ν_{as}(S–C), 628 ν_s(S–C), 512ν(S–S), 495, 477, 315, 285ν(S–Hg–S), 267, 121 ν(Hg–Br)

ν, stretching; δ, bending; ω, wagging

Table 4 The inhibition zone (mm) data values of the ligand and the complexes

Microorganisms/compounds	**1**	**2**	**3**	**4**	**5**	P10	AMP10	CTX30	VA30	OFX5	TE30	NY100	KET20	CLT10
Escherichia coli	12	13	22	14	16	18	12	10	22	30	28	–	–	–
Staphylococcus aureus	15	14	24	18	20	13	16	12	13	24	26	–	–	–
Klebsiella pneumoniae	11	10	16	12	13	18	14	13	22	28	30	–	–	–
Pseudomonas aeruginosa	14	12	18	14	15	8	10	54	10	44	34	–	–	–
Proteus vulgaris	14	11	12	14	13	10	16	18	20	28	26	–	–	–
Bacillus cereus	11	15	20	18	16	14	12	14	18	30	25	–	–	–
Mycobacterium smegmatis	12	11	16	13	14	15	21	11	20	32	24	–	–	–
Listeria monocytogenes	12	13	17	16	15	10	12	16	26	30	28	–	–	–
Micrococcus luteus	11	10	16	14	13	36	32	32	34	28	22	–	–	–
Candida albicans	14	14	22	15	18	–	–	–	–	–	–	20	21	15
Kluyveromyces fragilis	11	11	14	12	12	–	–	–	–	–	–	18	16	18
Rhodotorula rubra	13	12	20	14	18	–	–	–	–	–	–	18	22	16
Hanseniaspora guilliermondii	11	14	16	14	15	–	–	–	–	–	–	21	24	22
Debaryomyces hansenii	12	11	16	13	14	–	–	–	–	–	–	16	14	18

P10, Penicillin G (10 Units); AMP10, Ampicillin 10 μg; CTX30, Cefotaxime 30 μg; V30, Vancomycin 30 μg; OFX 5, Ofloxacin 5 μg; TE30, Tetracycline 30 μg; NY100, Nystatin 100 μg; KET20, Ketaconazole 20 μg; CLT10, Clotrimazole 10 μg

1, L; **2**, L·2HCl;**3**, Hg(L)Cl_2; **4**, Hg(L)Br_2; **5**, Hg(L)I_2

the formation of a neutral monometallic complexes (see experimental for conductivity values) probably having the distorted tetrahedral geometry [Hg(R–S–S–R)X_2] (X = Cl, Br, I) illustrated in Fig. 2. If the coordination occurs through sulphur atoms, one would expect that the vibrational frequencies for the CH_2(S–S)CH_2 unit and particularly for the (S–S) fragment will change significantly and most probably shifting to lower frequency region with respect to the free ligand [26–29]. However, in this comparison possible coupling of the ν(S–S) vibration with the ν(Hg–S) vibrations must also be considered which may lead to higher ν(S–S) values [30, 31]. On the other hand, if coordination occurs via nitrogen atoms, no considerable changes are expected in this region, apart from slight shifts in the characteristic imine frequencies. Based on these considerations, the band registered at 522 cm^{-1} (Raman) is (Fig. 5) assigned to the ν(S–S) frequency of the free ligand. Due to the nonpolar character of the S–S bond its counterpart in i.r. is quite weak and could be assigned at ca. 500 in the i.r. spectra (Fig. 6). The assignment is supported by the fact that the other relevant bands at 491, 539 cm^{-1} (Raman) and 500 cm^{-1} (i.r.) remain almost unchanged upon complex formation. The (S–S) stretches for the series $HgX_2(L)_2$ (X = Cl, Br, I) are expected to be on the one hand similar to that of the free ligand and on the other, comparable among each other. Therefore, the Raman bands of medium intensity observed at 510 (X = Cl), 508 (X = Br) and 512 cm^{-1} (X = I) are interpreted as ν(S–S) of the [Hg(L)X_2] complexes (Fig. 5). The i.r. spectra of [Hg(L)X_2] show also some weak absorptions in the respective wave range with the strongest ones located at 498 (Cl), 505 (Br) and 523 (I) cm^{-1} (Fig. 6). However, their assignment as the i.r. pendants of the aforementioned Raman bands is so far to be excluded, since the free ligand and the structurally related 1,3-bis(2-benzimidazyl)-2-thiapropane also exhibit infrared bands around 500 cm^{-1} [18, 22].

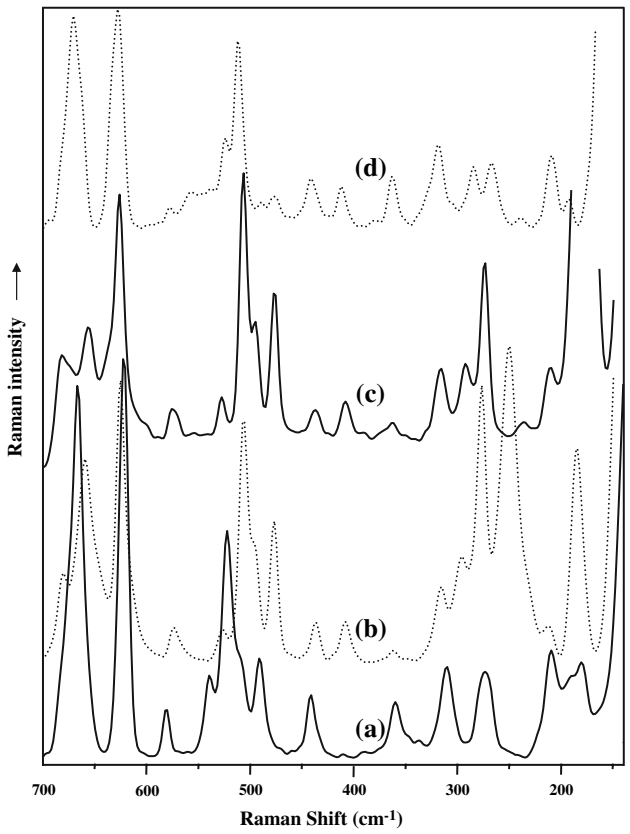

Fig. 5 Raman spectrum of **(a)** (L), **(b)** [Hg(L)Cl_2], **(c)** [Hg(L)Br_2] and **(d)** [Hg(L)I_2] in the 700–140 cm^{-1} region

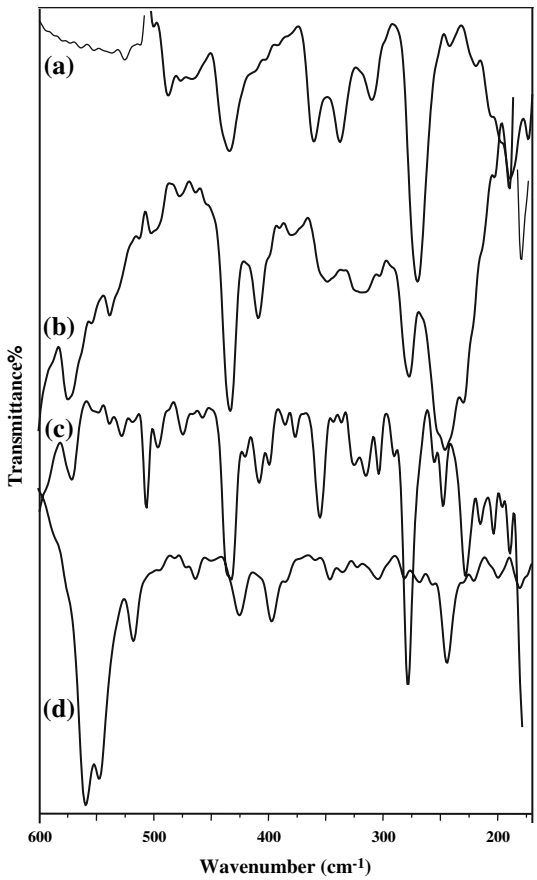

Fig. 6 Infrared spectrum of **(a)** (L), **(b)** [Hg(L)Cl_2], **(c)** [Hg(L)Br_2] and **(d)** [Hg(L)I_2] in the 600–170 cm^{-1} region

The shift of the ν(S–S) in the complex series [Hg(L)X_2] with respect to the free ligand L is in good agreement with the chemical softness of the elements, sulphur and mercury, indicating that the stronger Hg–S bond is clearly favoured over the weaker Hg–N interaction [32].

Only few reliable Raman vibrational data are available on tetrahedral mercury complexes with sulphur as donoring ligand. The symmetric stretching frequency ν(Hg–S) is expected to appear in the 400–200 cm^{-1} region as a band of

medium intensity both in Raman and i.r.: ν_s(Hg–S) = 255 and 276 cm^{-1} for the compounds HgS and $K_2[CH_3Hg(SCN)_3]$, respectively [33, 34]. Based on these data, the Raman bands registered at 298 [Cl], 292 [Br] and 284 cm^{-1} [I] are assigned to the symmetric stretches ν(Hg–S) in $HgX_2(L)_2$. The (Hg–S) frequencies show a slight shift to higher wavenumbers with respect to the literature values, probably resulting from the partial π character of the S–Hg–S chelation. On the other hand, the differences between the values for symmetric ν(Hg–S) in the title complexes are quite small. This, however, is expected since the high atomic mass of the central atom mercury allows only a weak vibrational coupling between the sulphide and halide vibrations. The antisymmetric (Hg–S) stretch should be best observed in the infrared spectrum. But, due to the low intensities and the superposition with the respective mercury halide vibrations no clear assignment could be made precisely.

In the case of mercury halides, an extensive vibrational spectroscopic data are available both for Raman and i.r., predominantly focused on the dihalides HgX_2 (X = F, Cl, Br, I) in gaseous, molten, matrix, or solid phases [35–39]. The Raman spectra of the solid HgX_2 series (X = Cl, Br, I) are illustrated in Fig. 7. The most intense bands appearing at 314 (Cl), 186 (Br) and 113 (I) cm^{-1} represent the symmetric stretches ν(Hg–X) [40–42]. The i.r. spectroscopical values for the solid HgX_2 are also reported: 374, 252 and 112 cm^{-1} for (Cl), (Br) and (I) respectively [43]. They correspond to the antisymmetric ν(Hg–X). The spectroscopical findings prove that the linear arrangement of the molecules are preserved to a great extend in the crystalline state. Slight but significant downshifts for ν(Hg–X) in the crystalline compounds results from strong van der Waals interactions between the molecules, which, in turn weakens the bonds and decreases the frequencies. However, in the present case, mercury is not linear but distorted tetrahedrally coordinated by two halogen and two sulphur atoms, so that the frequency values of the above mentioned mercury dihalides are only suitable for a rough comparison. More realistic are the data given for the tetrahalo mercurate series $[HgX_4]^{2-}$ with ν(Hg–X) cm^{-1}: 268(A_1)/229(F_2) (Cl), 164(A_1)/153(F_2) (Br) and 121(A_1)/120(F_2). In the Raman spectra of the $[Hg(L)X_2]$ complexes, the corresponding ν(Hg–X) frequencies are slightly shifted to 250, 175 and 121 cm^{-1} for Cl, Br and I ions, respectively. Once again, an important criterion for this assignment was that the remaining bands in the respective wave regions are present in the Raman spectrum of the free ligand, compared with all three $[Hg(L)X_2]$ complexes.

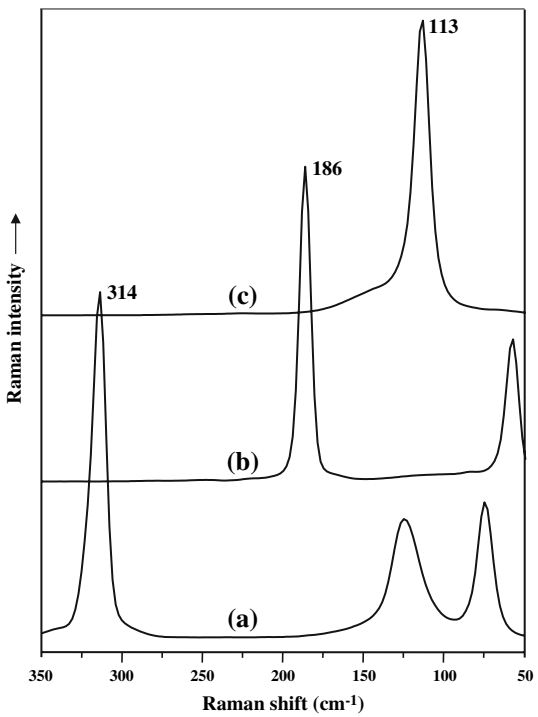

Fig. 7 Raman spectrum of **(a)** $HgCl_2$, **(b)** $HgBr_2$ and **(c)** [HgI_2 in the 350–50 cm^{-1} region

While the wave region $\nu < 300$ cm^{-1} is mainly characterized by the mercury halide and -sulphides modes, the range $\nu > 300$ cm^{-1} is exclusively dominated by the ring vibrations of the bis-imidazyl system of the ligand. The latter has been extensively studied and analysed previously [18].

In conclusion one may say, that the results of the conductivity measurements, as well as the vibrational spectroscopic and the nuclear magnetic resonance investigations confirm that the title complexes are neutral molecules in which the local geometry around the central mercury atoms corresponds to a distorted tetrahedron built up by two sulphur and two halogen atoms each (Fig. 7).

Antimicrobial activity

The results concerning in vitro antimicrobial activities of the ligand and the complexes together with the inhibition zone (mm) and (MIC) values of compared antibiotic and antifungal are presented in Tables 4 and 5. All the compounds tested exhibit strong or moderate antimicrobial activity. Of all the test compounds attempted, $Hg(L)Cl_2$ complex showed the highest activities against most Gram positive and Gram negative bacteria and as well as yeast cultures. As an example, 24 mm inhibition zone value on *Staphylococcus aureus* ($Gram^+$) organism for this compound is the highest effect compared with all the reference antibiotics, except tetracycline having the inhibition zone 26 mm on the same organism. Similarly this compound shows strong antifungal activity with the inhibition zone values 22 and 20 mm on *Candida albicans* and

Table 5 In vitro antimicrobial activity (MIC, μg mL^{-1}) of the ligand and complexes

Microorganisms/compounds	1	2	3	4	5	GEN	NYS
Escherichia coli	12.5	12.5	3.125	12.5	6.25	6.25	ND
Enterobacter aerogenes	6.25	6.25	3.125	6.25	6.25	3.125	ND
Staphylococcus aureus	6.25	6.25	1.56	3.125	3.125	25	ND
Klebsiella pneumoniae	50	50	6.25	25	12.5	6.25	ND
Bacillus cereus	25	6.25	3.125	3.125	6.25	6.25	ND
Micrococcus luteus	50	50	6.25	12.5	25	25	ND
Proteus vulgaris	12.5	25	25	12.5	12.5	6.25	ND
Mycobacterium smegmatis	25	25	6.25	12.5	12.5	12.5	ND
Listeria monocytogenes	25	25	6.25	6.25	12.5	12.5	ND
Pseudomonas aeruginosa	12.5	25	3.125	12.5	12.5	6.25	ND
Kluyveromyces fragilis	25	25	12.5	25	12.5	ND	6.25
Rhodotorula rubra	12.5	12.5	6.25	12.5	6.25	ND	6.25
Candida albicans	6.25	12.5	3.125	6.25	6.25	ND	3.125
Hanseniaspora guilliermondii	12.5	6.25	6.25	12.5	6.25	ND	3.125
Debaryomyces hansenii	25	25	6.25	12.5	12.5	ND	12.5

1, L; **2**, L·2HCl; **3**, $Hg(L)Cl_2$; **4**, $Hg(L)Br_2$; **5**, $Hg(L)I_2$. GEN, Gentamycin; NYS, Nystatin

ND, not determined

Rhodotorula rubra organisms, respectively. These values are consistent and compatible with all the antifungal in comparison tests. The MIC values in Table 5 indicate that all the compounds tested exhibit moderate to strong antimicrobial activity on the tested microorganisms. Once again the data indicate that the dichloride complex has a very strong and penetrating activity against most Gram positive and Gram negative bacteria and as well as yeast cultures. For instance, $Hg(L)Cl_2$ complex showed superior activity against *Staphylococcus aureus* ($Gram^+$) organism (MIC = 1.56 μg mL^{-1}) than the reference gentamycin (MIC = 25 μg mL^{-1}). This compound shows similar or improved antifungal activity against *C. albicans* (MIC = 3.125 μg mL^{-1}), *R. rubra* (MIC = 6.25 μg mL^{-1}) and *D. hansenii* (MIC = 6.25 μg mL^{-1}) than the reference nystatin (Table 5).

The inhibition activity seems to be governed to a certain degree by the facility of coordination at the mercury centre, because all three complexes are the most active against all tested micro-organisms, compared to the free ligands. It is known that zinc metallo-enzyme phosphomannose isomerase (PMI) plays an essential role in yeast cell wall biosynthesis and that this enzyme is inhibited by silver sulfadiazine, clinically used as a topical antibacterial and antifungal agent, through binding of metal centre with the Cysteine (sulphur containing amino acid) in proteins [44]. Taking the high affinity of the mercury centre with thiolate sulphur atoms into account, the mechanism of action of the mercury centre is plausibly similar to that of the silver agent. This supports the contention that certain binding or coordination most probably occur via certain section of microorganisms, causing the inhibition of biological synthesis and preventing the organisms from reproducing. Similarly, the reference tetracycline type antibiotics are thought to exert their antimicrobial effect by the inhibition of protein synthesis and ofloxacin (quinolones family) works by entering the bacterial cell and inhibiting DNA-gyrase, which is involved in the production of genetic material, preventing the bacteria from reproducing.

In classifying the antibacterial activity as Gram positive or Gram negative, it would generally be expected that a much greater number would be active against Gram positive than Gram negative bacteria [45]. However, in this study, the compounds are active against both types of the bacteria and as well as active against yeasts, which may indicate a broad-spectrum affect.

The results of our study indicate that the ligand and its halide salt have the potential to generate novel detoxification properties by displaying moderate to low affinities for most of the receptors. These compounds could be selected for further pharmacological tests to be evaluated as potential detoxification drugs against certain soft transition metal ions poisoning.

References

1. Rosenberg B (1980) Metal Ions in Biol Syst 1:1
2. Corey EJ, Mehrotra MM, Khan AU (1987) Science 236:68

3. Sadler PI (1991) Adv Inorg Chem 36:1
4. Bertini I, Gray HB, Lippard SJ, Valentine JS (1994) Bioinorganic chemistry. University Science Books, Sausalito
5. Patrick GL (2005) An introduction to medicinal chemistry, 3th edn. Oxford University Press
6. Giovagnini L, Marzano C, Bettio F, Fregona D (2005) J Inorg Biochem 99:39
7. Ma Y, Day CS, Bierbach U (2005) J Inorg Biochem 99:2013
8. Budakoti A, Abid M, Azam A (2006) Eur J Med Chem 41:63
9. Agh-Atabay NM, Dulger B, Gucin F (2005) Eur J Med Chem 40:1096
10. Tavman A, Agh-Atabay NM, Neshat A, Gucin F, Dulger B, Haciu D (2006) Trans Met Chem 31:194
11. Agh-Atabay NM, Dulger B, Gucin F (2003) Eur J Med Chem 38:875
12. Devereux M, Mc Cann M, Shea DO, Kelly R, Egan D, Deegan C, Kavanagh K, McKee V, Finn G (2004) J Inorg Biochem 98:1023
13. Aghatabay NM, Neshat A, Karabiyik T, Somer M, Haciu D, Dulger B (2007) Eur J Med Chem 42:205
14. Monthilal KK, Karunakaran C, Rajendran A, Murugesan R (2004) J Inorg Biochem 98:322
15. Irving H, Williams PJR (1953) J Chem Soc 3192
16. (a) Pearson RG (1963) J Am Chem Soc 85:3353; (b) Parr RG, Pearson RG (1983) J Am Chem Soc 105:7512
17. Addison AW, Burke PJ (1981) Heterocycl Chem 18:803
18. Agh-Atababy NM, Baykal A, Somer M (2004) Trans Met Chem 29:59
19. Performance standards for antimicrobial disk susceptibility tests (1993) Approved standard NCCLS publication M2-A5, Villanova, pp 1–32
20. Collins CH, Lyre PM, Grange JM (1989) Microbiological methods, 6th ed. Butterworth Co. Ltd., London
21. Jones RN, Barry AL, Gaven TL, Washington JA (1984) In: Lennette EH, Balows A, Shadomy WJ (eds) Manual of clinical microbiology, 4th edn. American Society for Microbiology, Washington, pp 972–977
22. Aghatabay NM, Somer M, Senel M, Dulger B, Gucin F (2007) Eur J Med Chem 42:1069
23. Yee KK, Barrow RF, Rogstad A (1974) J Chem Soc Faraday II 68:1105
24. Hopkins AG, Brown CW (1975) J Chem Phys 62:1598
25. Nakamoto K (1997) Infrared and Raman spectra of inorganic and coordination compounds, Part B, 5th edn. Wiley, p 200
26. Nakamoto K (1997) Infrared and Raman spectra of inorganic and coordination compounds, Part B, 5th edn. Wiley, p 199
27. Müller A, Jaegermann W, Enemark JH (1982) Coord Chem Rev 46:245
28. Chakrabarty PK, Bhattacharya S, Pierpont CG, Chakrabarty R (1992) Inorg Chem 31:3573
29. Guilard R, Ratti C, Tabard A, Richard P, Dubios D, Kadish KM (1990) Inorg Chem 29:2532
30. Müller A, Jostes R, Jaegermann W, Bhattacharyya RG (1980) Inorg Chim Acta 41:259
31. Müller A (1980) Analytical applications of FT-IR to molecular band biological systems. D Reidel, Dordrecht, p 257
32. Pearson RG (1968) J Chem Edu 45:581
33. Frost RL, Edwards HGM, Duong L, Kloprogge JT, Martens WN (2002) Analyst 127:293
34. Relf J, Cooney RP, Henneike HF (1972) Organomet Chem 39:75
35. Smith JH, Brill TB (1976) Inorg Chim Acta 18:225
36. Waters DN, Short EL, Thartwat M, Morris DFC (1973) J Mol Struct 17:389
37. Givan A, Loewenschuss A (1976) J Chem Phys 64:1967, ibid 65:1851
38. Loewenschuss A, Ron A, Schneep O (1969) J Chem Phys 50:2502
39. Givan A, Loewenschuss A (1978) J Chem Phys 68:2228
40. Nakashima S, Mishima H, Mitsuishi A (1973) Raman Spectrsc 1:325
41. Adams DM, Hopper MA (1971) Austr J Chem 24:885
42. Demiray AF (1977) Dissertation TU Clausthal Germany
43. Nyquist RA, Kagel RO (1971) Infrared spectra of inorganic compounds. Academic Press, New York, pp 423, 457, 475
44. Wells TNC, Scully P, Paravicini G, Proudfoot AEI, Payton MA (1995) Biochem 34:7896
45. McCutcheon AR, Ellis SM, Hancock REW, Towers GHN (1992) J Ethnopharmacol 37:213